

Ground State and Elementary Excitations of the $S = 1$ Kagomé Heisenberg Antiferromagnet

Kazuo HIDA *

Department of Physics, Faculty of Science,
Saitama University, Urawa, Saitama 338-8750
(Received February 19, 2007)

Low energy spectrum of the $S = 1$ kagomé Heisenberg antiferromagnet (KHAF) is studied by means of exact diagonalization and the cluster expansion. The magnitude of the energy gap of the magnetic excitation is consistent with the recent experimental observation for m -MPYNN·BF₄. In contrast to the $S = 1/2$ KHAF, the non-magnetic excitations have finite energy gap comparable to the magnetic excitation. As a physical picture of the ground state, the hexagon singlet solid state is proposed and verified by variational analysis.

KEYWORDS: kagomé Heisenberg antiferromagnet, Padé approximation, cluster expansion method, numerical diagonalization, hexagonal singlet solid state

§1. Introduction

The quantum antiferromagnets on the kagomé lattice has been extensively studied theoretically and experimentally because of the interest in the interplay of the strong quantum fluctuation and the highly frustrated nature of the lattice structure. So far, most of the attempts has been focused on the $S = 1/2$ case.¹⁻⁴ Owing to these extensive studies, it is widely accepted that the ground state of this model is a spin singlet state and the triplet excitation has a finite energy gap. Furthermore, there are a number of singlet excitations below the first triplet excitation possibly down to zero energy in the thermodynamic limit.⁴

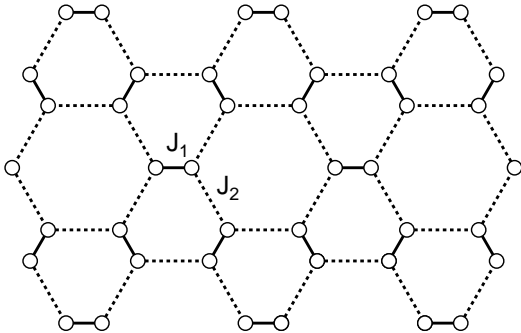


Fig. 1. The structure of m -MPYNN·BF₄ lattice.

Recently, Wada and coworkers⁵⁻⁷ have synthesized the material m -MPYNN·BF₄ and measured its magnetic and thermal properties. This material has the two dimensional structure which is schematically depicted in Fig. 1. Magnetically it can be regarded as the Heisenberg model consisting of dimers of two $S = 1/2$ spins on each *bond* of the triangular lattice. The intradimer exchange coupling J_1 is ferromagnetic and depicted by the thick solid lines. These spins are also coupled via inter-

dimer antiferromagnetic couplings J_2 represented by the thick dotted lines^{6,5,7}. Thus the Hamiltonian is given by,

$$H = J_1 \sum_{\text{intradimer}} \mathbf{s}_i \mathbf{s}_j + J_2 \sum_{\text{interdimer}} \mathbf{s}_i \mathbf{s}_j \quad (1.1)$$

where \mathbf{s}_i is the spin-1/2 operator. Experimentally, the exchange constants are estimated as $J_1 \simeq -23.26\text{K}$ and $J_2 \simeq 3.11\text{K}$ from susceptibility measurements, so that $|J_1| \gg |J_2|$. Therefore, at low temperatures, this material can be regarded as the spin-1 kagomé Heisenberg antiferromagnet (KHAF) described by the following Hamiltonian,

$$H = J \sum_{\langle i,j \rangle} \mathbf{S}_i \mathbf{S}_j \quad (1.2)$$

where \mathbf{S}_i is the spin-1 operator and the summation is taken over all nearest neighbour pairs of sites of the kagomé lattice. The effective exchange constant between $S = 1$ spins is given by $J = J_2/4 \simeq 0.78\text{K}$. Wada *et al.*⁵ confirmed that the magnetic excitation of this material has a finite energy gap $\Delta \simeq 0.25\text{K}$ from low temperature susceptibility measurement.

Theoretically, Asakawa and Suzuki⁸) have carried out the cluster expansion calculation for the ground state energy up to the fourth order in λ in their pioneering work. They calculated, however, the excitation gap only up to the first order so that conclusive result for the energy gap was not obtained.

In the present work, we investigate the ground state and excitation spectrum of this model (1.2) by the numerical diagonalization and series expansion method. We also propose a possible physical picture of the ground state named hexagon singlet solid (HSS) state. To confirm this picture, we perform the variational analysis of the ground state energy based on the HSS wave function.

This paper is organized as follows: In §2, the model Hamiltonian is presented. The numerical method em-

* e-mail: hida@phy.saitama-u.ac.jp

ployed in this work is explained in §3. The numerical results are presented in §4. The results are compared with experimental value for m -MPYNN-BF₄. The HSS picture of the ground state is presented in §5. The last section is devoted to a summary and discussion.

§2. Model Hamiltonian

Let us rewrite the Hamiltonian of $S = 1$ KHAF as follows,

$$\mathcal{H} = \mathcal{H}_u + \lambda \mathcal{H}_d, \quad (2.1)$$

$$\mathcal{H}_u = J \sum_{\triangle} \mathbf{S}_i \mathbf{S}_j, \quad (2.2)$$

$$\mathcal{H}_d = J \sum_{\nabla} \mathbf{S}_i \mathbf{S}_j, \quad (2.3)$$

where \sum_{\triangle} and \sum_{∇} represent the summation over the bonds in the upward pointed triangular clusters (UTC) and downward pointed triangular clusters (DTC), respectively, which are depicted in Fig. 2. Although we are interested in the uniform KHAF, we introduce the trimerization parameter λ for the computational purpose. In the following, we take the unit $J = 1$.

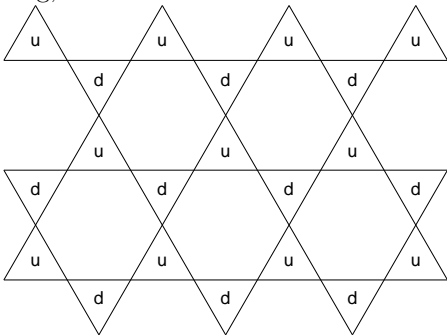


Fig. 2. Structure of the kagomé lattice. The UTC's and DTC's are denoted by u and d, respectively.

§3. Numerical Methods

3.1 Exact Diagonalization

For $N = 12, 15$ and 18 , the excitation energies of the low lying singlet and triplet excited states are calculated by the numerical diagonalization method using the Lanczos algorithm. The clusters shown in Fig. 3 are used with periodic boundary condition.

3.2 Cluster Expansion Method

As a complementary method, the magnetic excitation with $S = 1$ is calculated using the cluster expansion method treating \mathcal{H}_d as a perturbation.

Following Asakawa and Suzuki⁽⁸⁾, we take $\lambda = 0$ in the unperturbed state. In this case, the ground state is a simple assembly of independent singlet states on UTC. In the following, this state is called upward pointed triangular singlet (UTS) state and the corresponding state on DTC's is called downward pointed triangular singlet (DTS) state. We apply the series expansion with respect

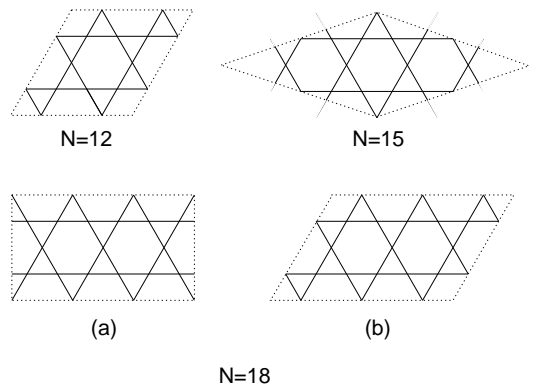


Fig. 3. The clusters used for numerical diagonalization.

to λ using the method of Gelfand, Singh and Huse^(9,10) and Gelfand⁽¹¹⁾ to obtain the series for the triplet excitation energy $\epsilon(\mathbf{k})$ up to the third order in λ where \mathbf{k} is the wave vector associated with the excitation.

$$\epsilon(\mathbf{k}; \lambda) = \sum_{m=0}^M c_m(\mathbf{k}) \lambda^m \quad \text{with } M = 3. \quad (3.1)$$

In general, it is practically impossible to check the convergence of this series. Actually, the energy gap evaluated from this series is in itself ill-behaved for $\lambda \gtrsim 0.3$. We therefore employ the Padé approximant,

$$\epsilon(\mathbf{k}; \lambda)^{[K,L]} = \frac{\sum_{k=0}^K p_k(\mathbf{k}) \lambda^k}{\sum_{l=0}^L q_l(\mathbf{k}) \lambda^l}, \quad (3.2)$$

with $p_0(\mathbf{k}) = 1$.

In the usual Padé approximation, $K + L$ must be equal to M . The original Hamiltonian (2.1), however, has the symmetry $H(1/\lambda) = H(\lambda)/\lambda$. Therefore the energy gap has also the same symmetry $\epsilon(\mathbf{k}; 1/\lambda) = \epsilon(\mathbf{k}; \lambda)/\lambda$. We therefore impose the same symmetry for the Padé approximant (3.2) which ensures $p_k = p_{K-k}$ and $q_l = q_{L-l}$ with $K = L + 1 = M$. In the following, we call this approximation as 'symmetric Padé approximation'. We also applied this approximation to the 4-th order series of the ground state energy per site ϵ_g obtained by Asakawa and Suzuki⁽⁸⁾ which yields the value $\epsilon_g = -1.4468$. This is close to the values estimated from exact diagonalization of $N = 18$ clusters, namely $\epsilon_g = -1.4511$ (cluster(a)) or -1.4393 (cluster(b)). This confirms the reliability of symmetric Padé approximation.

§4. Numerical Results

The λ -dependence of the energy gaps is shown in Fig. 4. According to the diagonalization results, the ground state is always the singlet state with total spin $S = 0$. The λ -dependence of the energy gap is common to all diagonalization data and series expansion data for small λ . For small λ , the lowest excitation has always $S = 1$. This corresponds to the triplet excitation localized in UTC. As λ increases, however, the properties of the lowest excited states vary depending on the methods used, size and form of the clusters. According to the diagonalization data, the singlet excitation with $S = 0$ comes

down as λ approaches unity. At $\lambda = 1$, the lowest excitation has $S = 1$ or $S = 0$ depending on the system size and forms of the cluster. They are summarized in table I. The first excited state has $S = 1$ for $N = 12$ and type (a) cluster with $N = 18$. On the other hand, for $N = 15$ and type (b) cluster with $N = 18$, the first excited state is $S = 0$ non-magnetic state. The magnetic gap and non-magnetic gap are close to each other for $N = 18$. As for the wave number of the excitations, most of the exact diagonalization data shows that the lowest excited state has wave number $\mathbf{k} = 0$ (Γ -point) except for the case of type (a) $N = 18$ cluster for which the magnetic gap is located at the K-point near $\lambda = 1$. On the other hand, the series expansion result shows that the magnetic gap is located at the W-point of the Brillouin zone for $\lambda > 0.48$ while it is located at the origin for $\lambda < 0.48$. The dispersion relation estimated from the series expansion is shown in Fig. 5.

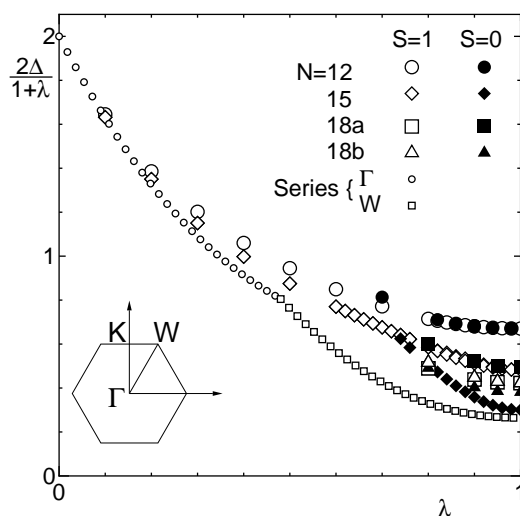


Fig. 4. The λ dependence of the energy gaps. The small symbols are the estimation from the symmetric Padé approximant of the cluster expansion series. The large symbols are the exact diagonalization results for $N = 12, 15$ and 18 , respectively. The inset is the Brillouin zone of the kagomé lattice. Energy gaps are normalized by a factor $(1 + \lambda)/2$ so that the symmetry $\Delta(1/\lambda) = \Delta(\lambda)/\lambda$ is evident.

Table I. Energy gap, spin quantum numbers and wave numbers of the low lying excited states of finite size clusters. The values with * are the lowest excitations for each cluster.

N	$\Delta(S = 0)$	k	$\Delta(S = 1)$	k
12	0.67074	0	0.67051*	0
15	0.30050*	0	0.48270	0
18a	0.49656	0	0.42262*	K-point
18b	0.38134*	0	0.42343	0

To make clear the difference between the excitation spectra of $S = 1/2$ and $S = 1$ KHAF, the system size dependence of the gaps are shown in Fig. 6(a) and (b)

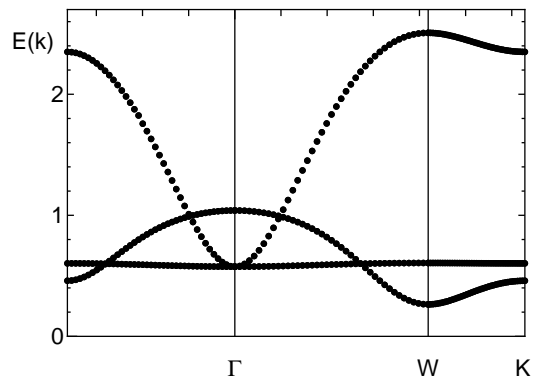


Fig. 5. The dispersion relation of $S = 1$ KHAF estimated from the symmetric Padé approximant of the cluster expansion series.

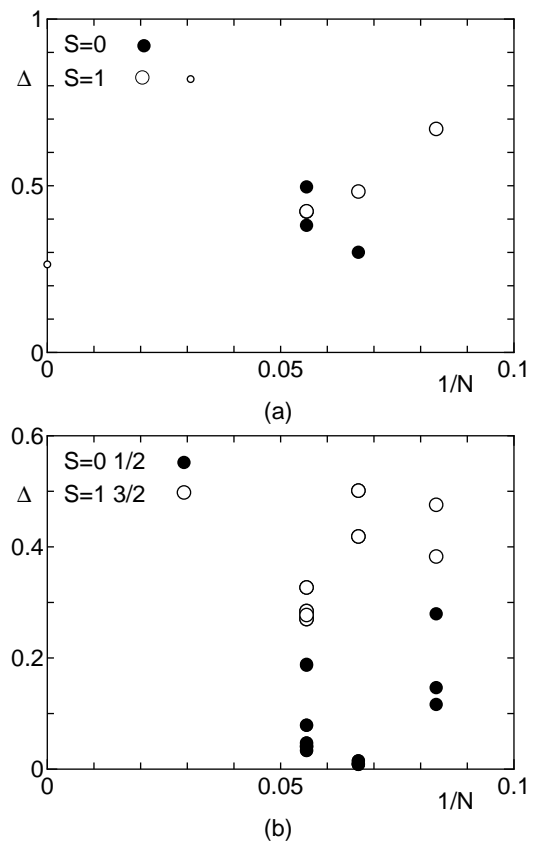


Fig. 6. The system size dependence of the energy gaps for $\lambda = 1$ for (a) $S = 1$ and (b) $S = 1/2$ KHAF. The small symbol in (a) is the estimation from the symmetric Padé approximant of the cluster expansion series. The large symbols are the exact diagonalization results. In (a), for $N = 12$ the filled circle is almost covered by the open circle.

for $S = 1$ and $S = 1/2$ cases, respectively. For $S = 1/2$ KHAF, the non-magnetic gap is much smaller than the magnetic gap. Actually, it is expected that the low energy non-magnetic excitations are distributed quasi-continuously down to zero according to the detailed calculation with larger clusters^{3,4}. For $S = 1$ case, however, both gaps have the same order of magnitude within the system sizes studied here and we find no indication of the appearance of the quasi-continuous non-magnetic

excitation spectrum.

As explained earlier, the values of the energy gaps depend considerably on the numerical methods used for their evaluation. Therefore it is not possible to estimate the precise value of the energy gap within the present calculation. Nevertheless, the numerically estimated magnetic gap lie between $0.42J$ ($N = 18$ cluster) and $0.26J$ (series expansion). These values are consistent with the magnetic gap of m -MPYNN·BF₄ which is estimated as $0.25\text{K} \simeq 0.32J$ from low temperature susceptibility measurement.

§5. Hexagon Singlet Solid Picture

The presence of finite magnetic gap suggests that the ground state consists of an assembly of localized singlet states. Apparently, there are three candidates of such singlet states. Two of them are UTS and DTS states which are the ground states for $\lambda = 0$ or $\lambda \rightarrow \infty$, respectively. At $\lambda = 1$, however, the symmetry between UTC's and DTC's is recovered. The ground state therefore should contain both states with equal weight.

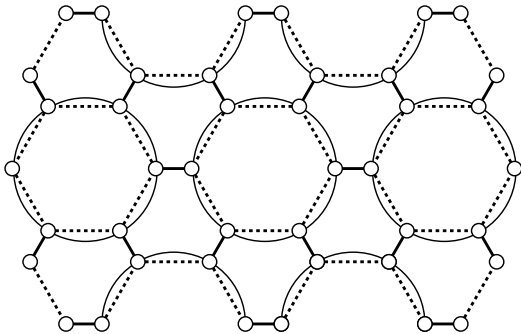


Fig. 7. The hexagon singlet solid state. The six $S = 1/2$ spins on a circle form a hexagon singlet state. The pairs of $S = 1/2$ spins connected by the thick solid lines are symmetrized to yield $S = 1$ spins.

There is another possibility that the singlet states are formed on the hexagonal clusters. Especially, if we decompose a $S = 1$ spin into two $S = 1/2$ spins, as in the VBS model of Haldane gap state¹²⁾, we can construct a trial state covered by local singlets without breaking the UTC-DTC symmetry as depicted in Fig. 7. Hereafter we call this state as hexagon singlet solid (HSS) state.

The wave function of the HSS state can be written down by expressing the single $S = 1$ spin state as,

$$\begin{aligned} |1\rangle &= \psi_{1/2,1/2}/\sqrt{2} \\ |0\rangle &= \psi_{1/2,-1/2} \equiv \psi_{-1/2,1/2} \\ |-1\rangle &= \psi_{-1/2,-1/2}/\sqrt{2} \end{aligned} \quad (5.1)$$

where $\psi_{\alpha,\beta}$ is the basis state of the $S = 1$ spin in terms of the two symmetrized $S = 1/2$ states defined as,

$$\psi_{\alpha,\beta} = [\psi_{\alpha} \otimes \psi_{\beta} + \psi_{\beta} \otimes \psi_{\alpha}]/\sqrt{2}. \quad (5.2)$$

Here ψ_{α} is the basis state of the $S = 1/2$ spin.

Following the construction of the VBS state by Affleck *et al*¹²⁾, we construct the HSS state as,

$$\begin{aligned} \Phi^{\text{HSS}} &= \bigotimes_i \psi_{\alpha_i,\beta_i} \prod_i (\delta_{\alpha_i,\gamma_i} + \delta_{\beta_i,\gamma_i}) \\ &\times \prod_p w^{\gamma_{i_p} \gamma_{j_p} \gamma_{k_p} \gamma_{l_p} \gamma_{m_p} \gamma_{n_p}} \end{aligned} \quad (5.3)$$

where the summation is assumed for the repeated indices. The i -th site has two $S = 1/2$ indices α_i and β_i . The index p distinguishes the hexagons and the sites $\{i_p, j_p, k_p, l_p, m_p, n_p\}$ belong to the p -th hexagon. The wave function $w^{\gamma_{i_p} \gamma_{j_p} \gamma_{k_p} \gamma_{l_p} \gamma_{m_p} \gamma_{n_p}}$ is that of the lowest singlet state of a single hexagon composed of six $S = 1/2$ spins.

Taking into account the two triangular singlet states Φ^{UTS} and Φ^{DTS} , we take the variational state as

$$\Phi = c_u \Phi^{\text{UTS}} + c_d \Phi^{\text{DTS}} + c_h \Phi^{\text{HSS}} \quad (5.4)$$

and minimize the energy expectation values for two types of clusters with $N = 18$ for $\lambda = 1$. As shown in table II, $c_u, c_d \ll c_h$ and the variational ground state energy is close to the exact value for both clusters. If we only admit two triangular singlet state, the variational energy per site is almost equal to -1 which is far from the exact value. On the other hand, if we take only the HSS state the variational energy is around -1.3 for both clusters. This value is already very close to the optimum value. Thus the HSS picture gives a reasonable physical picture of the ground state of $S = 1$ KHAF.

§6. Summary and Discussion

The spin-1 kagomé lattice antiferromagnetic Heisenberg model is studied by means of the cluster expansion and exact diagonalization method. The quantum numbers of the lowest excited state depends crucially on the method used, size and form of the clusters. This, in turn, confirms that the excitation spectrum of KHAF is strongly degenerate even for $S = 1$ case. It is suggested that the nonmagnetic excitations have finite energy gap as well as the magnetic excitations. The HSS picture of the ground state is presented and verified by the variational argument.

The material m -MPYNN·BF₄, which motivated the present study, can be regarded as the assembly of $S = 1/2$ spins on the hexagon as shown in Fig. 1. If the interhexagon coupling J_1 vanishes, the ground state is the six spin singlet state on each hexagon. If J_1 is switched on, the complete singlet state is perturbed. As far as J_1 is ferromagnetic, however, it cannot kill the spin degrees of freedom totally. Actually, we know that the $S = 1/2$ antiferromagnetic-ferromagnetic alternating Heisenberg chain has an energy gap even in the limit of infinitely strong ferromagnetic bond giving rise to the Haldane phase of the $S = 1$ Heisenberg chain.¹³⁾ From this analogy, also, it is reasonable that the magnetic gap remains finite in the present material even in the limit of $J_1 \rightarrow -\infty$ which is nothing but the $S = 1$ KHAF.

On the basis of HSS picture, we can also understand the physical origin of the finite non-magnetic gap in the following way. There are local singlet excited states in

Table II. Various estimations of ground state energy per site ϵ_g for $\lambda = 1$. The values estimated from variational function (5.4), pure HSS state, UTS+DTS state, numerical diagonalization and series expansion are tabulated. For the variational estimation, optimum values for the coefficients of HSS, UTS and DTS states are also shown.

Cluster	$\epsilon_g(\text{HSS+UTS+DTS})$	c_h	$c_u(=c_d)$	$\epsilon_g(\text{HSS})$	$\epsilon_g(\text{UTS+DTS})$	$\epsilon_g(\text{exact})$	$\epsilon_g(\text{series})$
18(a)	-1.3031	0.9921	0.0326	-1.3028	-1.0015	-1.4511	
18(b)	-1.3081	0.9966	0.0168	-1.3080	-1.0010	-1.4393	-1.4468

each single $S = 1/2$ hexagon. These states have the excitation energy of the same order of magnitude as the magnetic excitations. If J_1 is switched on, these states will tend to a gapped non-magnetic excitations.

Although the HSS picture seems to be a reasonable physical picture of the ground state of the $S = 1$ KAFH as stated above, in practice, we have chosen the series expansion scheme which starts from the UTS state. This is due to the following reasons: First, if we start from the hexagonal cluster of $S = 1/2$ spins, the expansion parameter is J_1 which tends to $-\infty$ in the limit of $S = 1$ KAFH. Therefore we have to estimate the series at the most unreliable point. Secondly, in the λ -expansion, we can take advantage of the symmetry between λ and $1/\lambda$ to improve the degree of Padé approximants. Lastly, the number of the states in a hexagonal cluster is much larger than that in a triangular cluster. Therefore we cannot calculate the higher order coefficients in the J_1 -expansion. From these viewpoints, we have chosen the λ -expansion scheme for the practical estimation of physical quantities.

This also implies that we obtained the results consistent with the HSS picture using the method which is not biased by the HSS picture. Therefore we may rather argue that our choice of the expansion scheme strengthens the reliability of the HSS picture. Nevertheless, it is also important to check if the series expansion based on the hexagonal cluster leads to the same conclusion. This is left for future studies.

The author thanks N. Wada for fruitful discussion and comments. The numerical calculation is performed using the FACOM VPP500 and HITAC SR8000 at the Supercomputer Center, Institute for Solid State Physics, the University of Tokyo, HITAC SR8000 at the Information Technology Center, the University of Tokyo and the HITAC S820/80 at the Information Processing Center, Saitama University. This work is supported by the Grant-in-Aid for Scientific Research from the Ministry of Education, Science, Sports and Culture.

- Y. Maruyama and N. Wada: Phys. Rev. **B49** (1994) 3975.
- 7) I. Watanabe, N. Wada, H. Yano, T. Okuno, K. Agawa, S. Ohira, K. Nishiyama, K. Nagamine: Phys. Rev. **B58** (1998) 2438.
- 8) H. Asakawa and M. Suzuki: Physica **A198** (1993) 210.
- 9) R. R. P. Singh, M. P. Gelfand and D. A. Huse: Phys. Rev. Lett. **60** (1988) 2484.
- 10) M. P. Gelfand, R. R. P. Singh and D. A. Huse: J. Stat. Phys. **59** (1990) 1093.
- 11) M. P. Gelfand: Solid State Comm. **98** (1996) 11.
- 12) I. Affleck, T. Kennedy, E. H. Lieb and H. Tasaki: Commn. Math. Phys. **115** (1988) 477; Phys. Rev. Lett. **59** (1987) 799..
- 13) K. Hida: Phys. Rev. **B45** (1992) 2207.

-
- 1) C. Zeng and V. Elser: Phys. Rev. **B42** (1990) 8436.
 - 2) N. Elstner and A. P. Young: Phys. Rev. **B50** (1994) 6871.
 - 3) T. Nakamura and S. Miyashita: Phys. Rev. **B52** (1995) 9174.
 - 4) Ch. Waldtmann, H.-U. Everts, B. Bernu, C. Lhullier, P. Sindzingre, P. Lecheminant and L. Pierre: Eur. Phys. J. **B2** (1998) 501.
 - 5) N. Wada, T. Kobayashi, H. Yano, T. Okuno, A. Yamaguchi and K. Agawa: J. Phys. Soc. Jpn. **66** (1997) 961.
 - 6) K. Agawa, T. Okubo, A. Yamaguchi, M. Hasegawa, T. Inabe,